Journal of Marine Science and Technology

Volume 26 | Issue 4 Article 1

ANALYSIS OF POWER SYSTEM LOW FREQUENCY OSCILLATION WITH EMPIRICAL MODE DECOMPOSITION

Chia-Liang Lu
Department of Electrical Engineering, National Taiwan Ocean University, Keelung, Taiwan, R.O.C

Chia-Yu Hsu
Department of Electrical Engineering, National Taiwan Ocean University, Keelung, Taiwan, R.O.C.

Pei-Hwa Huang
Department of Electrical Engineering, National Taiwan Ocean University, Keelung, Taiwan, R.O.C,
b0104@mail.ntou.edu.tw

Recommended Citation

Lu, Chia-Liang; Hsu, Chia-Yu; and Huang, Pei-Hwa (2018) "ANALYSIS OF POWER SYSTEM LOW FREQUENCY OSCILLATION WITH EMPIRICAL MODE DECOMPOSITION," *Journal of Marine Science and Technology*: Vol. 26: Iss. 4, Article 1.
DOI: 10.6119/JMST.201808_26(4).0001
Available at: https://jmstt.ntou.edu.tw/journal/vol26/iss4/1

Journal of Marine Science and Technology, Vol. 26, No. 4, pp. 477-486 (2018)
DOI: 10.6119/JMST.201808_26(4).0001

ANALYSIS OF POWER SYSTEM LOW FREQUENCY OSCILLATION WITH EMPIRICAL MODE DECOMPOSITION

Chia-Liang Lu, Chia-Yu Hsu, and Pei-Hwa Huang

Key words: power system stability, low frequency oscillation, empirical mode decomposition, time-frequency analysis.

ABSTRACT

The low frequency oscillation (LFO) in power systems often consists of composite responses of various oscillation modes. Thus a direct analysis of LFO for revealing system dynamic characteristics is not straightforward. The primary objective of this study is to utilize the method of empirical mode decomposition (EMD) to expand the LFO response under study into multiple intrinsic mode functions (IMFs) for detailed investigation of power system dynamics. Then time-frequency power information is explored using wavelet transform to obtain time-frequency power graph which is further resolved into a time-frequency-power diagram. Finally, information from the time-frequency-power diagram is further examined to determine those generators that demonstrate higher degree of participation in the LFO of power system. The comparative analysis in frequency domain shows that, at specific frequencies in LFO modes, higher oscillation participation power also shows a larger participation factor in its frequency domain analysis.

I. INTRODUCTION

A practical response is something that can be described and analyzed in the time and frequency domains. Analysis of the time domain enables one to understand the intuitive changes of a response (amplitude) over time, whereas the analysis of the frequency domain provides understanding of how response amplitude varies with frequency. Compared to time domain response analysis, frequency domain analysis is more intuitive and convenient.

An objective of response analysis is to describe basic response characteristics and expressions. The most crucial and fundamental variables used in response analysis are time and frequency. In the field of conventional response processing, a Fourier transform-based response domain expressions and its domain distribution of power show the response characteristics in that frequency domain. These characteristics have been used extensively throughout the development of conventional response analysis and processing. However, Fourier transform is an overall transform; its representation of a response is entirely in the time domain or entirely in the frequency domain. Subsequently, power spectrums for frequency domain expressions are unable to show the occurrences or transform conditions of certain frequency quantities. In actuality, the majority of response frequencies change over time; consequently, to determine the global response characteristics in just a time domain or a frequency domain is insufficient. Thus, the goal of this research is to obtain information about changes of response's frequencies in a spectrum over time. Time-frequency analysis (Cohen, 1995; Qian, 1996; Qian and Chen, 1999; Grochenig, 2001) has been used to simultaneously show the change process of frequency and amplitude over time. We would thus be able to comprehensively identify the characteristics and structure of the response.

For the analysis of low frequency oscillation (LFO) in power system, the systemic response obtained using time domain methods is the integrated responses from various oscillation modes; thus, it is difficult to determine the characteristics of each mode. Previous studies have complemented this analysis with frequency domain analytical methods. The LFO issues have been examined from the perspective of small signal stability through linear processing of system state equations. System linearization is typically conducted at the point of operation to obtain a linear model of the system. The stability problem is analyzed in the frequency domain and its attributes become a problem that requires solving eigenvalues and eigenvectors; the oscillation frequency and damping size of each oscillation mode could be determined using the eigenvalue, whereas the range and degree of effect on the system caused by oscillation modes (i.e., mode shape) is identified using the eigenvector. However, power systems are non-linear. The degree of complexity of power system progressively increases in conjunction with system scale. Thus, the linearization method frequently becomes limited by system scale and/or equation order (Chang, 1993b; Anderson and Fouad, 1994; Kundur, 1994; Pardiyar, 1995; Pai, 2000; Rogers, 2000;

Paper submitted 12/05/13; revised 03/21/14; accepted 03/25/14. Author for correspondence: Pei-Hwa Huang (e-mail: b0104@mail.ntou.edu.tw).
Department of Electrical Engineering, National Taiwan Ocean University, Keelung, Taiwan, R.O.C.

Pai et al., 2004; Messina, 2009).

Short-time Fourier transform and wavelet transform are frequently employed for time-frequency analysis (Cohen, 1995; Rao, 1998; Tapan, 2002). These methods have specific advantages and disadvantages. Short-time Fourier transform of a response is influenced significantly by window functions while different window functions produce different analysis results. For wavelet transform, the basic wavelet function cannot be changed after it has been determined. This potentially causes mutual overlap of adjacent frequencies in local responses, thereby obstructing the identification of frequency.

The Empirical Mode Decomposition (EMD) method is suitable for improving situations of mal-adaptation experienced with wavelet transform (Huang et al., 1998; Huang et al., 1999; Messina, 2009). Wavelet transform analysis uses the same basis functions for its calculations, regardless of response changes. Therefore, the physical significance is only obtained for linear physical phenomena. However, EMD uses the internal time scale of the data change for a direct analysis of energy. The response is expanded into multiple intrinsic mode functions (IMFs). These functions are then used as the basis for response expansion. This process is based entirely on the characteristics of the original response, which could display non-linear characteristics.

The primary purpose of this study is the integration of time and frequency domains. We employ time-frequency analysis to analyze the LFO of power system and understand the characteristics displayed by oscillating response frequencies that change over time. Change process in transient information, such as oscillation frequency, time of fault occurrences, and power of oscillation frequency, are subsequently obtained using time-frequency graphs, and are further compared with those of the frequency domain to verify the accuracy of the time-frequency analysis.

II. FREQUENCY AND TIME DOMAIN SIMULATION

LFO is primarily used to analyze system responses under minor disturbances. The frequency domain analytical method (Chang et al., 1993a; Anderson and Fouad, 1994; Kundur, 1994; Huang, 2002) can be applied to directly determine various oscillation modes within a system. Therefore, it is suitable for obtaining a linear system model by system linearization at the point of operation. The stability problem is analyzed within the frequency domain so that its attributes become problems that require the solving of eigenvalues and eigenvectors; the oscillation frequency and damping size of each oscillation mode can be obtained using eigenvalue, whereas the range and degree of effect exerted on the system by each oscillation mode are shown by eigenvectors. This is the oscillation mode shape.

The system eigenvalue and eigenvector have been collectively termed as the eigenstructure (Huang, 1989; Huang, 2002). Once the eigenstructure of the system is obtained, the dynamic stability of the entire system can be understood. When LFO involves numerous response units, their individual degrees of participation and causes of oscillation are obtainable through complete system analysis. Time domain simulations methods are commonly employed to verify frequency domain analysis results (Chang et al., 1993a). The system's dynamic model is initially used in collaboration with the initial system conditions and changes or disturbances in the system state. The mathematical model's differential equations for system dynamics are solved using integrals to simulate the system dynamic response following a disturbance. This method of analysis requires numerous tests to as-certain the system response stability caused by various disturbances. In addition, the system response obtained is generally a sum of responses from various oscillation modes; thus, it becomes difficult to determine the damping effect of each oscillation mode. Therefore, time domain simulations are used complementarily with frequency domain analysis. This is the most frequently used method in the investigation of topics related to dynamics of power system.

III. TIME-FREQUENCY ANALYSIS

1. Empirical Mode Decomposition (EMD)

The process of EMD involves the decomposition of complex responses into limited individual Intrinsic Mode Function (IMF), thereby bestowing a physical meaning to actual responses (Huang et al., 1998; Huang et al., 1999). IMFs have the following characteristics:

(1) In the whole data set, the number of extrema and the number of zero-crossings must either be equal or differ at most by one.
(2) At any point, the mean value of the envelope defined by the local maxima and the envelope defined by the local minima is zero.

The EMD is able to resolve power directly from the internal time scales of data changes. The initial response data is expanded into multiple IMFs. These functions are then used as the basis for expansion or for the analysis of non-linear response. Thus, the physical characteristics of the original response can be displayed in its entirety.

Through EMD, the internal time scale of data changes is used to directly determine response power. The response is represented as a summation of multiple IMFs. The IMFs are regarded as the basis for response expansion. In the IMFs, oscillation amplitude of the first component is the greatest and at the highest frequency. The subsequent oscillation amplitude and frequency of the IMF components become progressively lower. The power involved in oscillation also becomes reduced.

2. Wavelet Transform

Wavelets are defined as wave morphologies that show average wave amplitude values of zero at a specific wavelength. Through the extension and compression of wavelet functions, an analyzed response can be expanded. Wavelet transform made use of wavelet functions formed by parameters such as scale and shift to describe the response; the scale parameter size shows the high

and low changes in frequency, and the shift parameter provides time-related information. Therefore, information concerning time and frequency domains is obtainable. Previous studies have divided wavelet transform into continuous and discrete wavelet transform (Cohen, 1995; Rao, 1998; Tapan, 2002). Continuous wavelet transform can be expressed as:

$$\psi_{a,b}(t) = \frac{1}{\sqrt{a}}\psi\left(\frac{t-b}{a}\right) \tag{1}$$

where a is the scale parameter and b is the shift parameter. Following conditions of the discretization restrictions, the two parameters are solved as

$$a = a_0^j,\ b = ka_0{}^j b_0,\ j \in Z \tag{2}$$

By substituting (2) into (1), the discrete wavelet function can be expressed as:

$$\psi_{j,k}(t) = a_0^{\frac{-j}{2}}\psi\left(a_0^{-j}t - kb_0\right) \tag{3}$$

The discrete wavelet transform coefficient for continuous response $x(t)$ can be expressed as:

$$C_{j,k} = a_0^{\frac{-j}{2}}\int_{-\infty}^{\infty} x(t)\ \psi\left(a_0^{-j}t - kb_0\right)dt \tag{4}$$

If the samples obtained for continuous response $x(t)$ is discrete response $x[n]$, then the discrete wavelet transform coefficient can be expressed as:

$$C_{j,k} = a_0^{\frac{-j}{2}}\sum_n X[n]\ \psi^*\left[a_0^{-j}t - kb_0\right] \tag{5}$$

The initial response $x[n]$ could also be expressed through wavelet transform as:

$$x[n] = a_0^{\frac{-j}{2}}\sum_j\sum_k C_{j,k}\ \psi\left[a_0^{-j}n - kb_0\right] \tag{6}$$

From (6), it can be seen that manipulating the size of a_0 and b_0, the wavelet transform is capable of displaying various time and frequency resolutions. The most commonly used parameters for the average wavelet transform is $a_0 = 2$ and $b_0 = 1$.

III. EMD IN COLLABORATION WITH WAVELET TRANSFORM

Although wavelet transform is able to reflect changes in response characteristics over time by integrating time and frequency domains during the construction of the time-frequency response characteristics, its analysis is based on the same wavelet function; thus, the separation rate is limited. This also causes a decrease in the resolution power during the analysis. The level of response complexity from non-linear power system increases in conjunction with system scale. This further reduces the resolution of wavelet analysis.

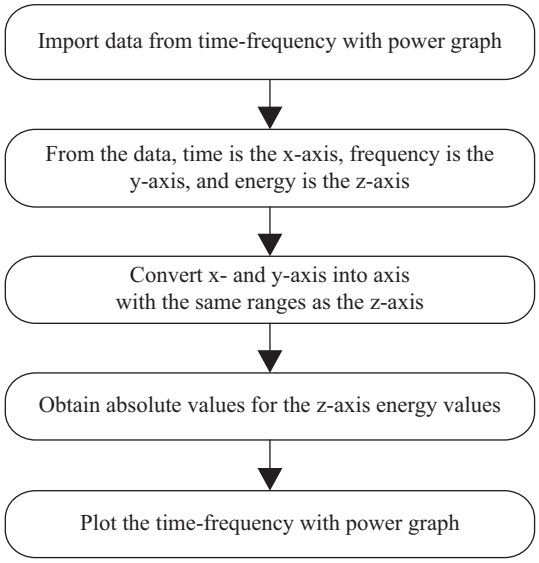

Fig. 1. Flowchart of the process of transforming the time-frequency with power graph into a time-frequency with power graph.

EMD represents the response as the summation of multiple IMFs. Each IMF is based on its own internal time scale. Therefore, the problem of choice or appropriateness of base does not occur. This also improves the performance of wavelet transform in the time-frequency method.

This study opts to use the system power response during a power system fault as the starting point for EMD. The response IMF is decomposed. The first and second IMF components, where amplitude is the greatest, are subject to wavelet transform to produce a time-frequency with power graph. The data from the time-frequency with power graph are exported and processed to transform the time-frequency with power graph into a time-frequency- power graph. The process is shown in Fig. 1. Finally, data from the time-frequency-power graph are analyzed to determine the primary LFO frequency and characteristics of the power system. Fig. 2 shows the flowchart of the system analytical method.

IV. CASE STUDIES

1. The Study System

A four-machine two-area power system is used as the study system for this work. This system comprises two areas (Areas A and B), and four Generators (G_1 and G_2 in Area A; G_3 and G_4 in Area B). The single-line diagram of this system is shown in Fig. 3 (Kundur, 1994).

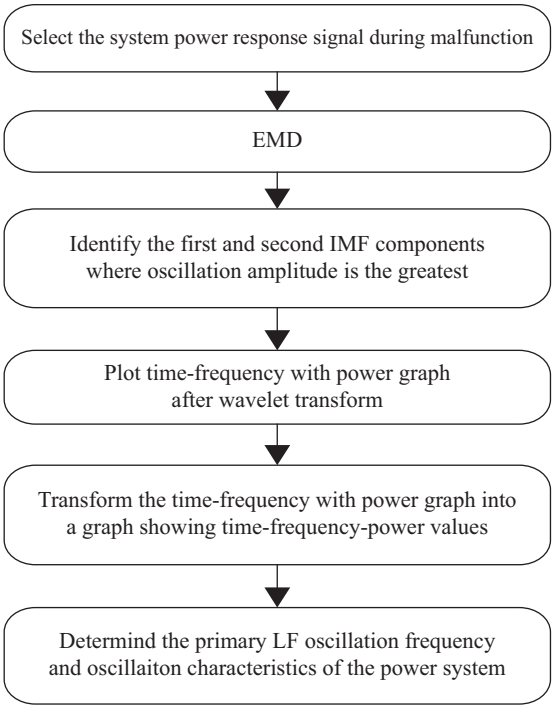

Fig. 2. Flowchart of the system analysis process.

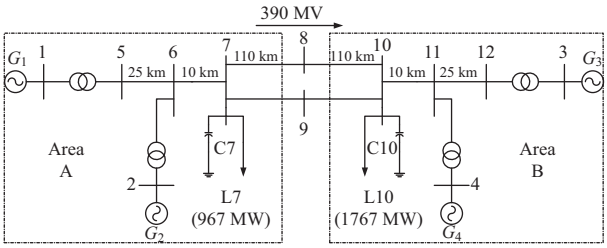

Fig. 3. Single-line diagram of the two-area power system. (Kundur, 1994).

The total installation capacity of the system is 3600 MVA. Each Generator is connected to a step-up transformer to increase voltage from 20 to 230 kV. Areas A and B are connected by two lines. Each Generator's rated capacity is 900 MVA, with a rated voltage of 20 kV. Area A transmits 390 MW to Area B. Each step-up transformer resistance $0 + j0.15$ pu is based on 900 MVA, 20/230 kV. The nominal voltage for the system is 230 kV. The resistance parameters of the transmission line are as follows: $r = 0.0001$ pu/km, $L_X = 0.001$ pu/km and $b_c = 0.00175$ pu/km. The operating conditions for the Generators within the system are as follows:

$G_1 \quad P = 700$ MW $\quad Q = 185$ Mvar $\quad E_t = 1.03\angle 20.2°$

$G_2 \quad P = 700$ MW $\quad Q = 235$ Mvar $\quad E_t = 1.01\angle 10.5°$

$G_3 \quad P = 719$ MW $\quad Q = 176$ Mvar $\quad E_t = 1.03\angle -6.8°$

$G_4 \quad P = 700$ MW $\quad Q = 202$ Mvar $\quad E_t = 1.01\angle -17°$

Table 1. Information pertaining to power flow in each area.

Area		Generation	Load	Bus Shunt	Charging	Net INT	Losses
Area A	P (MW)	1400.0	967	0.0	0.0	390.3	42.7
	Q (Mvar)	450.9	100	-182.4	20.2	-47.9	601.3
Area B	P (MW)	1420.2	1767.0	0.0	0.0	-390.3	43.5
	Q (Mvar)	412.0	100.0	-325.8	20.4	47.9	610.3
Total	P (MW)	2820.2	2734.0	0.0	0.0	0.0	86.2
	Q (Mvar)	862.9	200.0	-508.2	40.6	0.0	1211.6

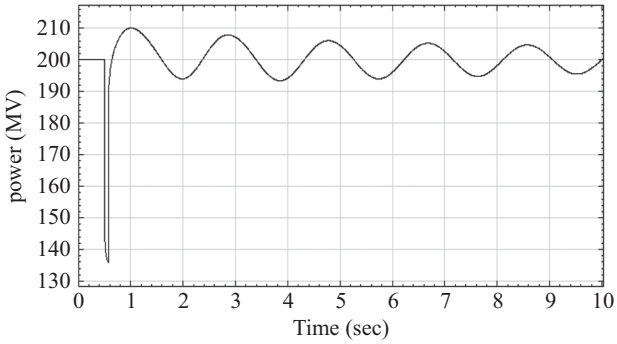

Fig. 4. Power response graph for transmission line between Bus 7 and Bus 8.

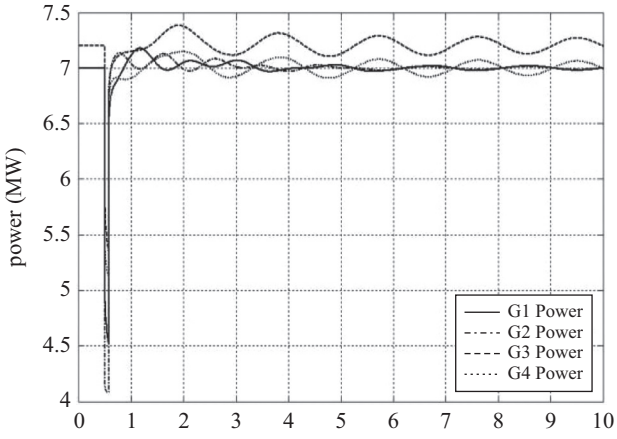

Fig. 5. Power response graph for system Generators G_1,G_2, G_3, and G_4.

Bus 7 of Area A is attached a load of $P_L = 967$ MW, $Q_L = 100$ Mvar, and $Q_C = 200$ Mvar, and Bus 10 of Area B is attached a load of $P_L = 1767$ MW, and $Q_C = 350$ Mvar. The information pertaining to power flow in each area is shown in Table 1 (Kundur 1994).

2. Time-Frequency Analysis

The system analysis includes an application of a three-phase fault on Bus 9 at the time of 0.5 s and cleared after four cycles. System dynamic response is simulated for ten seconds. The power responses from each generator and transmission line are recorded. After time-frequency analysis, the oscillation fre-

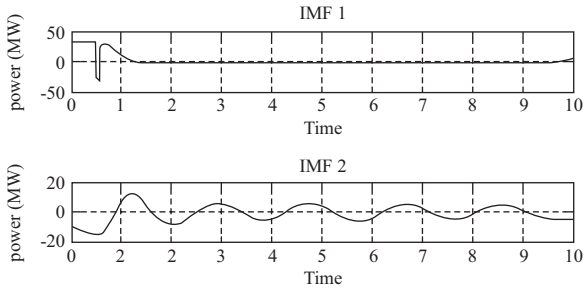

Fig. 6. IMF composition for the power of transmission line between Bus 7 and Bus 8.

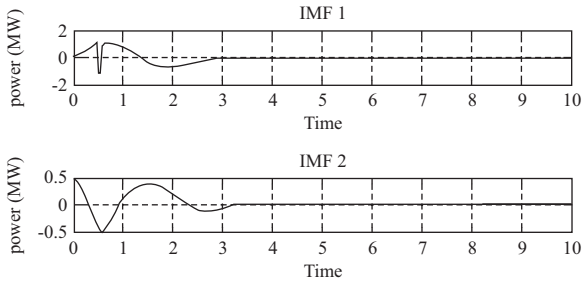

Fig. 7. IMF composition for the power of Generator G_1.

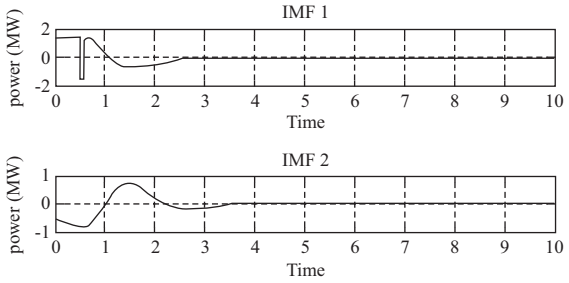

Fig. 8. IMF composition for the power of Generator G_2.

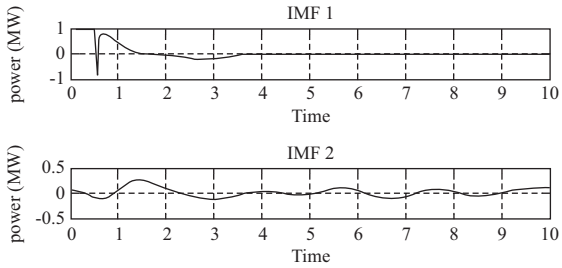

Fig. 9. IMF composition for the power of Generator G_3.

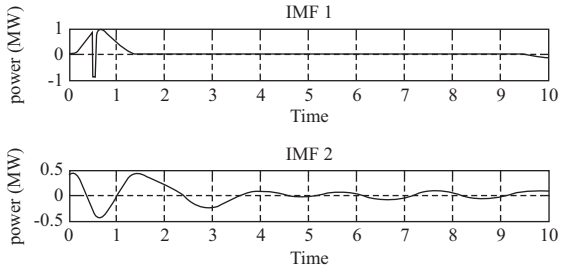

Fig. 10. IMF composition for the power of Generator G_4.

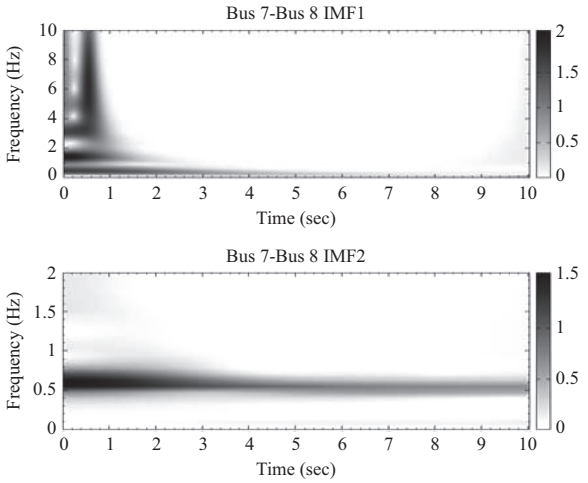

Fig. 11. Time-frequency with power graphs after wavelet transform of IMF1 and IMF2 for transmission line between Bus 7 and Bus 8.

quency and characteristics of each response is determined. The accuracy of the results obtained from the time-frequency analyses are verified by comparison with the frequency domain analysis results.

3. No Installation of Power System Stabilizer

Transmission line between Bus 7 and Bus 8 and Generators G_1, G_2, G_3, and G_4 are observed. Figs. 4 and 5 show the power responses during system fault.

After EMD, the power response, transmission line between Bus 7 and Bus 8, and Generators G_1, G_2, G_3, and G_4 are expanded into a summation of IMFs, as shown in Figs. 6-10 which are based on MW power units. The graphs in Figs. 6-10 show that the power responses from each generator and transmission line which are time- varying after system fault is cleared. The graphs for the IMF2s in Figs. 9 and 10 reveal that the IMF responses of Generators G_3 and G_4 are in continuous oscillation.

The first and second components (IMF1 and IMF2, respectively) in Figs. 6-10 show time-frequency with power graphs as shown in Figs. 11-15 that are based on MW power units. The graphs in Figs. 11-15 show that the frequency with power responses from each generator and transmission line are time varying. Through wavelet transform, Figs. 14 and 15 show that Generators G_3 and G_4 produce frequencies between 0.5 and 0.6 Hz during 8 s to 10 s, indicating the presence of larger power responses.

Frequency composition from time-frequency with power graphs cannot be clearly analyzed; therefore, the graphs shown in Figs. 11-15 are exported and processed to transform the time-frequency with power graphs into time-frequency-power graphs, as shown in Figs. 16-20 which are based on MW power units.

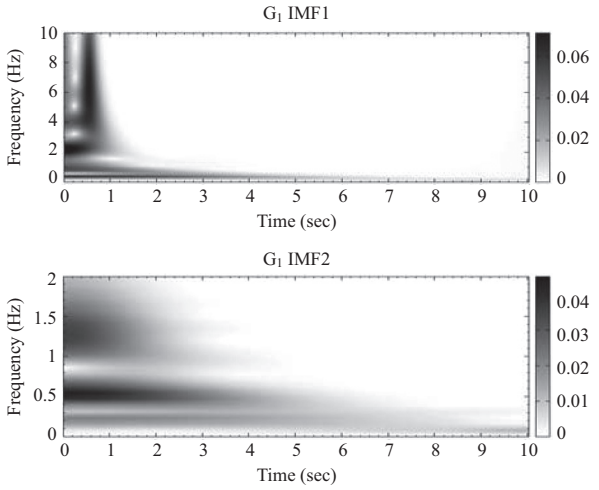

Fig. 12. Time-frequency with power graphs after wavelet transform of IMF1 and IMF2 for Generator G_1.

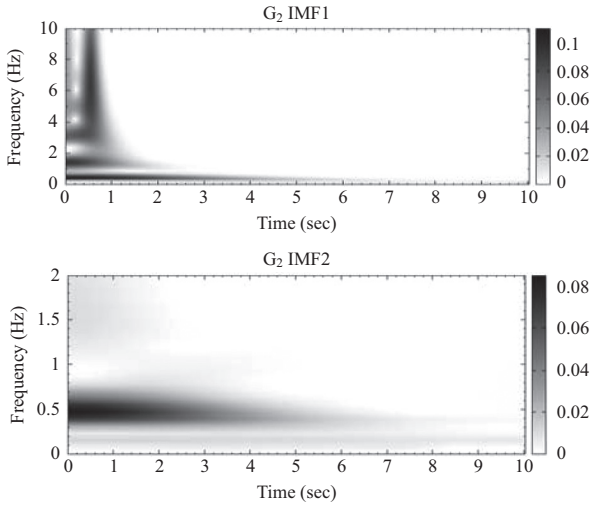

Fig. 13. Time-frequency with power graphs after wavelet transform of IMF1 and IMF2 for Generator G_2.

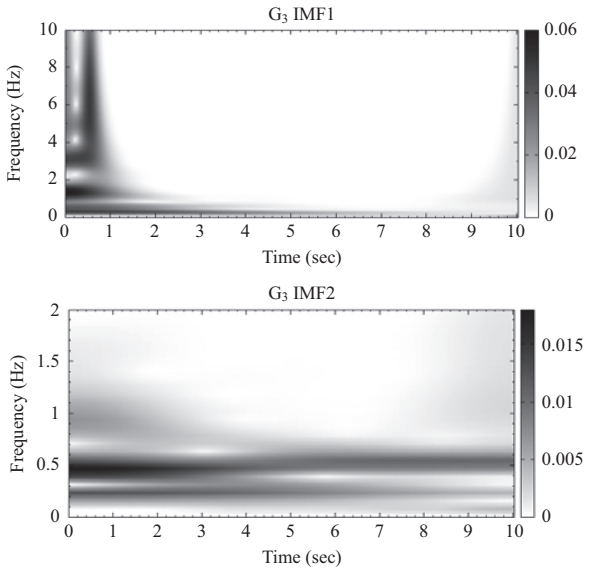

Fig. 14. Time-frequency with power graphs after wavelet transform of IMF1 and IMF2 for Generator G_3.

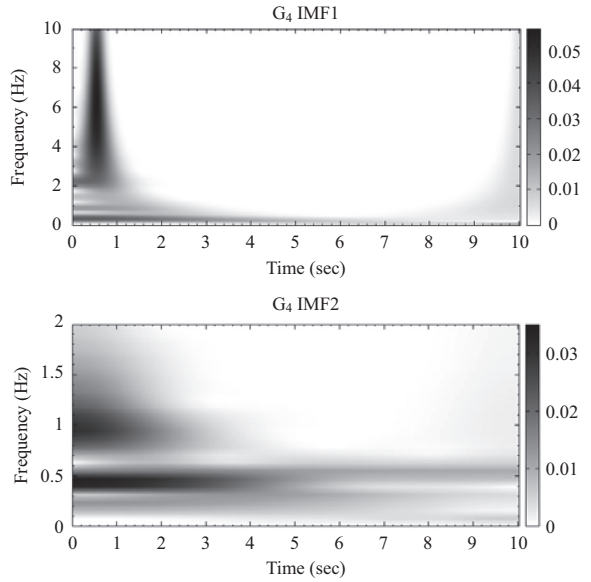

Fig. 15. Time-frequency with power graphs after wavelet transform of IMF1 and IMF2 for Generator G_4.

The graphs in Figs. 16-20 show that all the frequencies with power oscillation which consist of power responses from each generator and transmission line are time-varying. From these graphs, the continuous oscillation response could be determined. Its frequency and the amplitude of its power could be determined.

From the data revealed by Figs. 16-20, the primary LFO frequency and characteristics of the power system can be investigated. Table 2 shows relevant information obtained from the above analysis.

The graphs shown in Figs. 12-15 and the data in Table 2 allow the following conclusions to be made:

(1) The first component in the IMF graph obtained from the EMD expansion should be the transient response that occurs during fault of a power system and not the power system LFO.

(2) IMF2 of transmission line between Bus 7 and Bus 8, and Generators G_1, G_3, and G_4 show a constant frequency of 0.5512 Hz over an extended period. Figs. 14 and 15 show that the oscillations at Generators G_3, and G_4 are most significant, persisting for up to 10 s. Therefore, it is hypothesized that this frequency is the oscillation frequency for the Inter-Area mode of the system.

(3) The 0.5512 Hz response persisted for longer at Generators G_3 and G_4 than at G_1 and G_2. Thus, the frequency's power becomes comparatively larger with the slower decaying over time. Under the oscillation mode at this frequency, Genera-

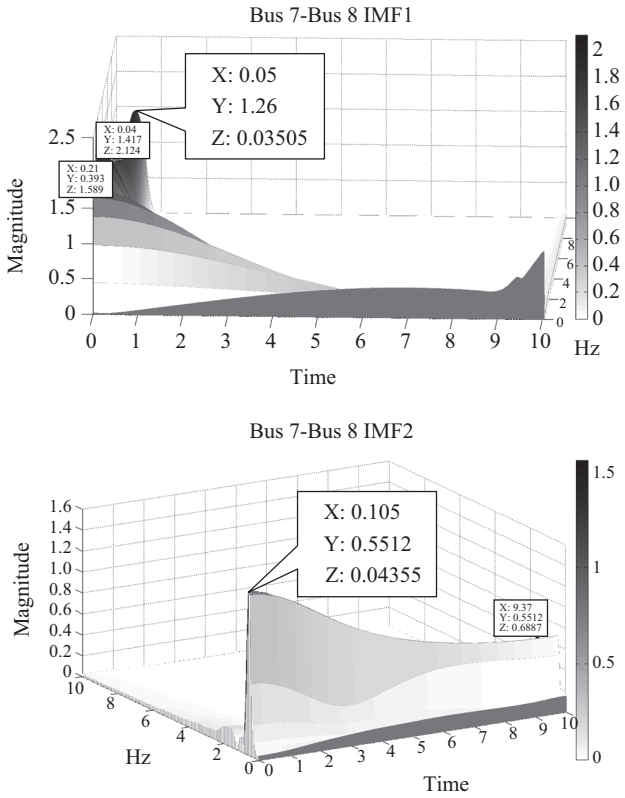

Fig. 16. Time-frequency with power graphs of IMF1 and IMF2 for transmission line between Bus 7 and Bus 8.

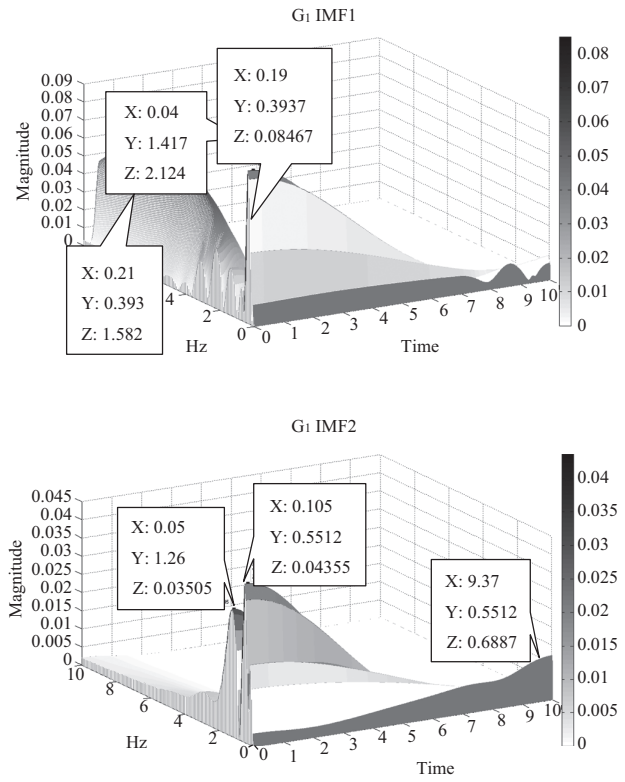

Fig. 17. Time-frequency with power graphs of IMF1 and IMF2 for Generator G_1.

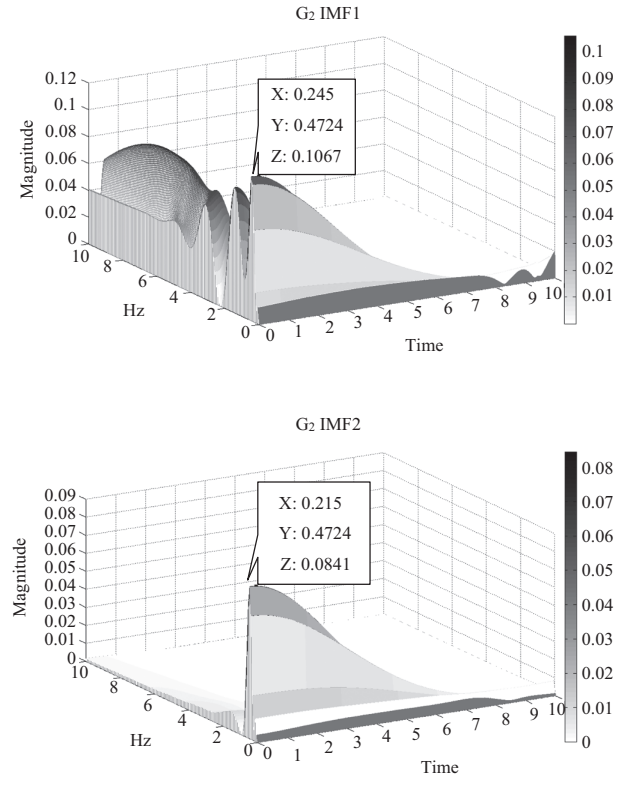

Fig. 18. Time-frequency with power graphs of IMF1 and IMF2 for Generator G_2.

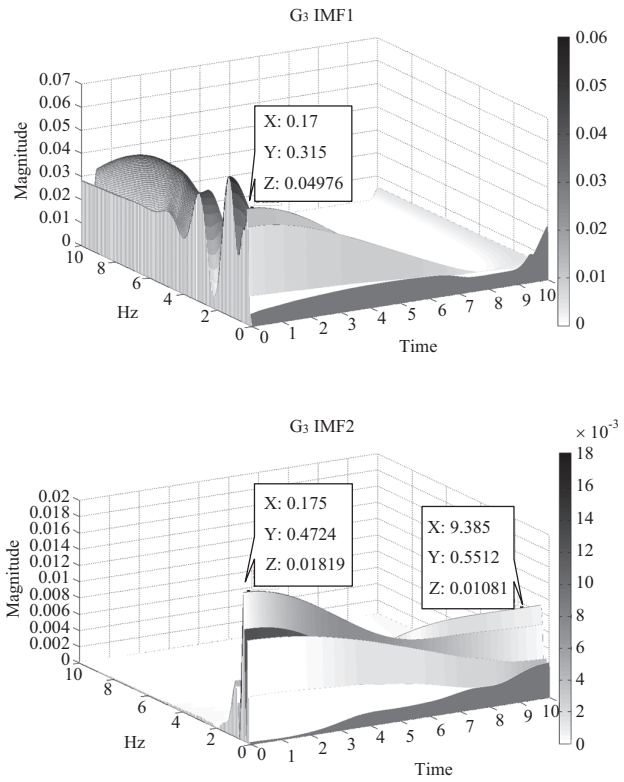

Fig. 19. Time-frequency with power graphs of IMF1 and IMF2 for Generator G_3.

Table 2. The primary LFO frequency (Hz) of IMF component for transmission line and each Generator.

	IMF1	IMF2
transmission line between Bus7 and Bus8	0.3937, 1.417	0.5512
Generator G1	0.3937	0.5512, 1.26
Generator G2	0.4724	0.4724
Generator G3	0.315	0.4724, 0.5512
Generator G4	0.315	0.3937, 0.5512

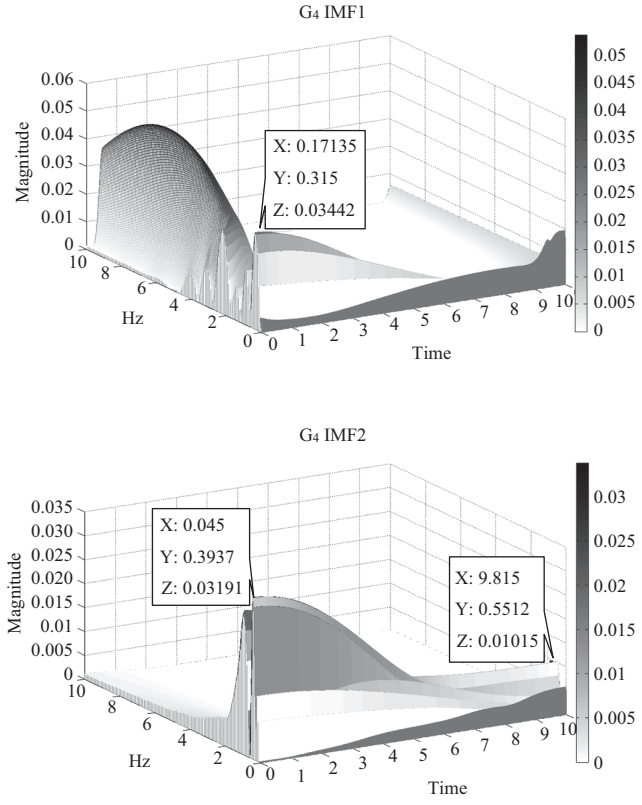

Fig. 20. Time-frequency with power graphs of IMF1 and IMF2 for Generator G_4.

tors G_3 and G_4 show a greater involved oscillation power than G_1 and G_2. Generator G_3 is the highest.

The following section discusses the installation of power system stabilizer for Generators G_1, G_2, G_3, and G_4, as well as the consequent system damping response improvements. This is used to determine the installation positions the power system stabilizer (PSS).

4. Installation of Power System Stabilizer

Power system stabilizer is installed on Generators G_1, G_2, G_3, and G_4. The PSS gain is set at 40 to observe the transmission line between Bus 7 and Bus 8 response improvements. Figs. 21-24 show the power responses from PSS installed on Generators G_1, G_2, G_3, and G_4, respectively.

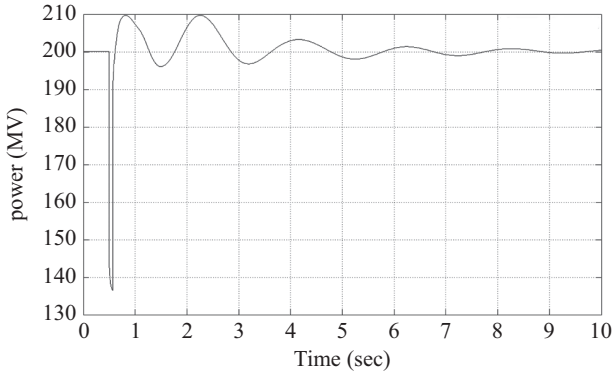

Fig. 21. Power response of transmission line for PSS installed on Generator G_1.

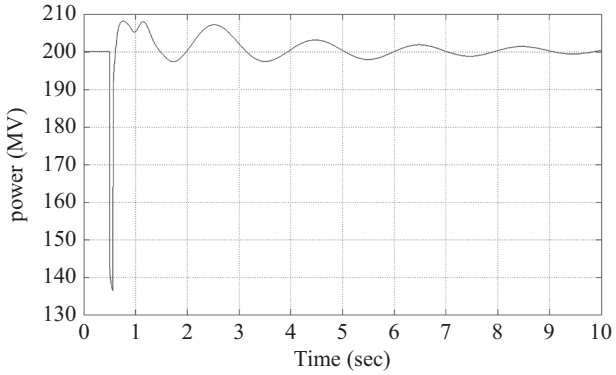

Fig. 22. Power response of transmission line for PSS installed on Generator G_2.

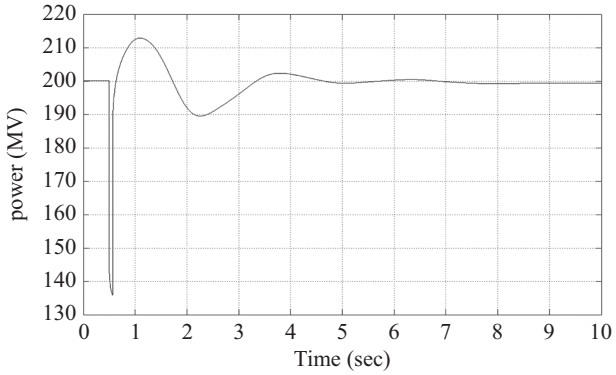

Fig. 23. Power response of transmission line for PSS installed on Generator G_3.

The power response graphs show that the installation of power system stabilizer significantly improves system damping. This improvement is especially prominent for Generator G_3. The amplitude after 10 s of system fault is more restrained compared to those of Generators G_1, G_2, and G_4 with PSSs.

The LFO eigenvalues of the two-area power system are shown in Table 3. The right eigenvector and participation factor of LFO Mode 3 (the inter-area mode) in Table 3 are shown in Table 4.

Table 3. LFO eigenvalues of two-area power system.

Mode	Eigenvalue	Damping ratio	Frequency (Hz)
1	-0.59943 ± *j*6.7829	0.088031	1.0795
2	-0.58674 ± *j*6.5804	0.088813	1.0473
3	-0.050451 ± *j*3.3142	0.015221	0.52747
4	-0.55086 ± *j*0.63185	0.65715	0.10056
5	-0.87916 ± *j*0.51586	0.84619	0.082102
6	-0.40638 ± *j*0.36101	0.74761	0.057456
7	-0.39057 ± *j*0.35934	0.73591	0.057191

Table 4. Right eigenvector and participation factor of Mode 3.

Mode variable	Right Eigenvector		Participation factor
	Size	Phase (°)	
$\Delta\omega(G_3)$	1.0000	0.0000	1.00000
$\Delta\omega(G_4)$	0.91134	-0.29350	0.70239
$\Delta\omega(G_1)$	0.25781	173.98	0.25757
$\Delta\omega(G_2)$	0.17870	175.39	0.13546

The graphs in Figs. 7-10 and Figs. 21-24 as well as the data shown in Tables 2-4 allow the following conclusions to be made:

(1) Figs. 7-10 and Tables 2 to 3 indicate a 0.5512 Hz response in IMF2 of Generators G_1, G_3, and G_4 before PSS is installed which persisted for an extended amount of time. This is especially evident for Generators G_3 and G_4 where the response persisted for longer than 10 s.
(2) Figs. 7-10 and Table 2 show that a 0.5512 Hz response persisted for longer at Generators G_3 and G_4 than those that occur at Generators G_1 and G_2. The power of this frequency is large and its decaying over time is slow. This shows that the power involved with oscillation for Generators G_3 and G_4 under the oscillation mode at this frequency are greater than those of Generators G_1 and G_2. Generator G_3 has the highest energy.
(3) Figs. 7-10 and Table 4 show that the greater the participation factor of Generator G_3, the greater its power involved with oscillation and the longer the time oscillation continues.
(4) Figs. 21-24 show that the installation of PSS significantly improves system damping. This improvement is especially evident when PSS are installed on Generator G_3. In this case, the amplitude is more restrained 10 s after fault than for PSS installed on Generator G_1, G_2, and G_4.

V. CONCLUSION

Time-frequency analysis is capable of representing time-frequency with power responses in the form of 3D time-frequency-power graphs. This shows the abundance of frequency components contained within the response and how the power of each frequency component changes over time. Compared to frequency domain analysis, time domain analysis additionally has the time

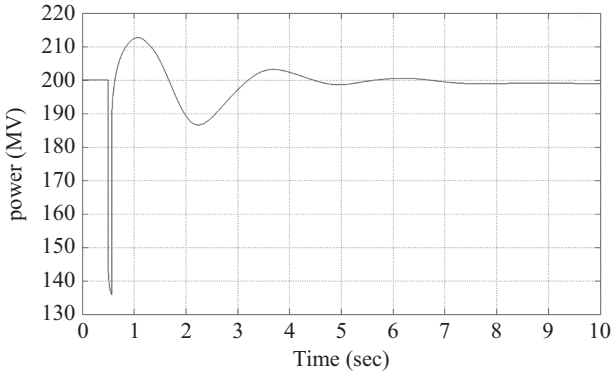

Fig. 24. Power response of transmission line for PSS installed on Generator G_4.

data of the response. This enables it to realize the duration that a frequency occurs and the conditions of its power decaying. This makes observation and research of power system responses more convenient.

This study utilizes EMD to decompose power responses into IMFs. The IMFs are subsequently subjected to wavelet transform to obtain time-frequency with power graphs. The time-frequency with power graphs are then exported and processed into time-frequency-power graphs. Consequently, a realistic representation of the process of response change is obtained. The following conclusions can be made based on the analysis results:

(1) A multitude of oscillation frequencies are included in the system's power responses. EMD is employed to expand the responses into multiple IMFs. Through this process, influences on high frequency transient responses are reduced. Furthermore, the interference experienced when observing IMF is also reduced. This simplified the observation of each oscillation frequency.
(2) The oscillation of Inter-Area modes has a broad area of influence. It also comprises more components. At each observation point, frequencies could be observed in the majority of cases. The power of the frequency is thus comparatively greater and persists longer.
(3) The frequency of Inter-Area oscillation modes as observed using time-frequency graphs of generators, showing that units with higher oscillation participation power that decays at a slower rate over time has higher participation factor values.
(4) With specific reference to the Inter-Area oscillation modes, units with high participation factor values are equipped with PSS. The analytical results from the time and frequency domain analyses show a significant effect in providing damping to the system, and thus the system stability is improved.

REFERENCES

Anderson, P. M. and A. A. Fouad (1994). Power System Control and Stability. IEEE Press.

Chang, C. L., A. S. Liu and C. T. Huang (1993a). Oscillatory stability analysis using real-time measured data. IEEE Transactions on Power Systems 3,

823-829.
Chang, C. L. (1993b). Research and improvement of low frequency oscillation of Taipower system. Monthly Journal of Taipower's Engineering 540, 5-8. (in Chinese)
Cohen, L. (1995). Time-Frequency Analysis. Prentice Hall PTR.
Grochenig, K. (2001). Foundations of Time-Frequency Analysis. Birkhauser.
Huang, P. H. (1989). Power System Dynamic Stability Study Via Eigenstructure Analysis. Ph.D. Dissertation, Department of Electrical Engineering, National Taiwan University, Taipei, Taiwan. (in Chinese)
Huang, N. E., Z. Shen, S. R. Long, M. C. Wu, H. H. Shih, Q. Zheng, N. C. Yen, C. C. Tung and H. H. Liu (1998). The empirical mode decomposition and the Hilbert spectrum for nonlinear and non-stationary time series analysis. Proceedings of the Royal Society of London 454, 903-995.
Huang, N. E., Z. Shen and S. R. Long (1999). A new view of nonlinear water waves: The Hilbert spectrum. Annual Review of Fluid Mechanics 31, 417-457.
Huang, N. E., M. C. Wu, S. R. Long, S. P. Shen, W. Qu, P. Gloersen and K. L. Fan (2003). A confidence limit for the empirical mode decomposition and Hilbert spectral analysis. Proceedings of Royal Society of London 459, 2317-2345.
Huang, N. E. and N. O. Attoh-Okine (2005a). The Hilbert-Huang Transform in Engineering. Taylor & Francis.
Huang, N. E. and S. S. P. Shen (2005b). Hilbert-Huang Transform and Its Applications. World Scientific.
Huang, P. H. (2002). Calculation method for critical eigenvalue of power system small signal stability. Electricity Monthly 4, 282-289. (in Chinese)
Kundur, P. (1994). Power System Stability and Control. McGraw-Hill.
Messina, A. R. (2009). Inter-Area Oscillations in Power Systems. Springer.
Pai, M. A. (2000). Power System Oscillations. Kluwer Academic Publishers.
Pai, M. A., D. P. S. Gupta and K. R. Padiyar (2004). Small Signal Analysis of Power Systems. Narosa Publishing House.
Pardiyar, K. R. (1995). Power System Dynamics Stability and Control. John Wiley & Sons.
Qian, S. (1996). Joint Time-Frequency Analysis: Methods and Applications. Prentice Hall PTR.
Qian, S. and D. Chen (1999). Joint time-frequency analysis. IEEE Signal Processing Magazine 16, 52-67.
Rao, R. M. (1998). Wavelet Transforms: Introduction to Theory and Applications. Addison-Wesley.
Rogers, G. (2000). Power System Oscillations. Kluwer Academic.
Tapan, K. (2002). Wavelet Applications in Engineering Electromagnetics. Artech House.